Ain Shams Engineering Journal (2017) 8, 571–580

Ain Shams University

Ain Shams Engineering Journal

www.elsevier.com/locate/asej
www.sciencedirect.com

ELECTRICAL ENGINEERING

Design and implementation of a low-cost maximization power conversion system for brushless DC generator

Abolfazl Halvaei Niasar *, **AmirHossein Sabbaghean**

Faculty of Electrical & Computer Engineering, University of Kashan, Kashan, P.O. Box: 87317-51167, Iran

Received 30 August 2015; revised 22 October 2015; accepted 1 November 2015
Available online 27 November 2015

KEYWORDS

Brushless DC generator;
Permanent magnet synchronous generator;
Power density maximization;
Active rectifier;
Current shaping

Abstract This paper presents a simple and low-cost method to capture maximum power throughput of permanent magnet brushless DC (BLDC) generator. Conventional methods of rectification are based on passive converters, and because the current waveform cannot be controlled as ideal waveform, a highly distorted current is drawn from brushless generator. It leads to lower power factor and reduces the efficiency and power per ampere capability. So, in this study an active six-witch power converter is employed and based on the phase back-EMF voltage, an optimum current waveform is generated. The phase currents are controlled inphase to phase voltages and their magnitudes are adjusted to regulate the DC-link voltage. Proposed control theory is verified by simulations for BLDC generator and permanent magnet synchronous generator (PMSG). Moreover, some experimental results are given to demonstrate the theoretical and simulation results.

1. Introduction

Nowadays, developments in distributed generating systems as well as propulsion systems for electric and hybrid electric vehicles have significantly increased the popularity of permanent magnet (PM) brushless generators. These types of generators have been used in various applications such as automotive, micro-turbines, wind power generation, due to their high power density, robustness, and reliability [1]. There are two main types of PM brushless generators: trapezoidal type (BLDCG) and sinusoidal type (PMSG). The PMSGs need high resolution position sensors for optimal operation if the modern vector based control techniques were employed, whereas BLDCGs just need three low-cost Hall-effect position sensors [2]. Compared with other generators, BLDC generator has the advantages of light weight, compact design, easier control, and low maintenance [3,4]. The BLDC generator can have approximately 15% higher power density compared with a PM synchronous generator [5]. On the other hand, due to variable frequency of output voltage caused by variable speed of the generator's shaft in many isolated generation systems such as wind energy conversion systems (WECS) or automotive applications, power electronics interfaces are provided for

* Corresponding author. Tel.: +98 31 55912412.
E-mail addresses: halvaei@kashanu.ac.ir (A.H. Niasar), asabbaghian68@gmail.com (A. Sabbaghean).
Peer review under responsibility of Ain Shams University.

Production and hosting by Elsevier

http://dx.doi.org/10.1016/j.asej.2015.11.001

Nomenclature

e_a, e_b, e_c	stator phase back-EMF voltages
H_1, H_2, H_3	output signal of Hall Effect position sensors
i_a, i_b, i_c	stator phase currents
I'_a	reference phase current in negative slope part
L_s	stator inductance per phase
M	stator mutual inductance
P_{avg}	airgap power average
P_{output}	output power of generator
R_s	stator resistance per phase
$t_{H_1,off}$	falling edge instant of sensor H_1
$t_{H_1,on}$	rising edge instant of sensor H_1
$t_{H_2,off}$	falling edge instant of sensor H_2
$t_{H_2,on}$	rising edge instant of sensor H_2
v_a, v_b, v_c	stator terminal voltages
BLDCG	brushless direct current generator
EV	electric vehicle
EMF	electro-motive force
FFT	fast Fourier transformation
HEV	hybrid electric vehicle
PM	permanent magnet
PMDC	permanent magnet direct current
PMSG	permanent magnet synchronous generator
WECS	wind energy conversion system

PM brushless generators. The most important issue in this system is the extraction of maximum electrical power from generator at the lower losses, which reduces the size and weight of the generator [6]. Fig. 1 shows various employed topologies for BLDC generation system.

The simplest solution is the using of uncontrolled three-phase rectifiers as shown in Fig. 1(a) that doesn't need any control and has the lowest cost. In this case, the back-EMF magnitude of the generator must be higher than the DC bus capacitor voltage, which varies because it depends on generator speed and on the DC load. Hence, the output power depends on both speed and load resistance. Therefore, the topology with an uncontrolled rectifier presents relatively low efficiency and low power density [7]. Due to mentioned shortages in some applications, BLDC generators are controlled using diode bridge with DC/DC converter topology as shown in Fig. 1(b). By adding diode bridge to any BLDC generator, different DC/DC converters may be employed with regulation of voltage, current or power. Main reason for exploiting such solution is due to its simplicity and modular design. However, one of the main drawbacks of this topology is highly distorted uncontrolled current in the AC side gives low power per ampere. In this topology, the phase voltages and currents of BLDCG are not inphase, and so the power factor is reduced [8].

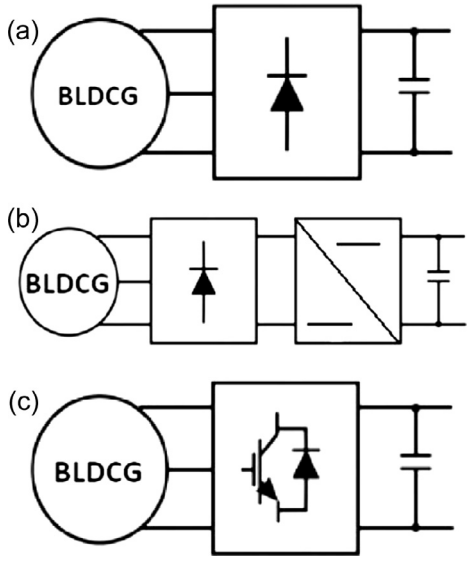

Figure 1 Various BLDC generator topologies (a) passive rectifier, (b) active rectifier and (c) passive rectifier cascaded with DC/DC converter.

Another solution is the use of power converter with six active switches as shown in Fig. 1(c) [9,10]. Various control strategies such as vector based, current waveform shaping and current optimization strategies can be employed for this topology. It seems that this makes control hardware of variable speed generator complex and expensive, but results in outstanding performance for small shaft speeds of the drive. This complex system can be found in regenerative braking applications in electric and hybrid vehicles. On this way, the maximum power per ampere is extracted from BLDC generator [11]. The direct power control strategy has been used for voltage and power regulation of BLDC generator system [12]. In [13] a current control method has been proposed to eliminate torque ripple and maximize power density of non-sinusoidal BLDC machines for EVs and HEVs. On this way, for specific harmonic elimination, a simple algebraic method has been employed instead of FFT. A predictive control of a brushless DC generator based on simultaneously minimization of torque ripple and joule losses has been presented in [14]. A hybrid permanent magnet (HPM) generator has been used at fixed rotor speed passive filter to generate a variable DC-link voltage for hybrid electric vehicle in [15]. The machine excitation is controlled to capture the desired power and voltage. Foregoing problems due to current distortion has been solved with a complex system. Another BLDCG based power supply system using passive rectifier has been used for small-scale WECS in [16], in which for DC-link voltage regulation a DC/DC converter has been used. In [17] a BLDCG based wind energy conversion system for distribute electric power generation has been employed. A PWM rectifier is used for controlling the BLDCG power and the reference phases' currents are as rectangular.

This paper develops analysis and implementation of a new current shaping algorithm for BLDC generator. Developed algorithm can be designed for maximum power extraction or DC voltage regulation. Proposed system may be used for WECS, regenerative braking in automotive systems and micro-turbine based power supply systems. After description

of BLDC generator drive system, a new optimal power control is developed for BLDC generator based and then, some simulations and experiments are given to demonstrate proposed control algorithm.

2. Optimal power control for BLDC generator

2.1. BLDC generator system and modeling

In order to simplify the three-phase control and maximize the output power, an equivalent dynamic model of BLDCG is derived. The equivalent circuit of the BLDC generator is shown in Fig. 2. It is assumed that phases' resistances and inductances of three windings are equal, induced phase back-EMF voltages have an identical shape; switches and core losses are negligible [5]. With these assumptions, the phase voltage equations of BLDC generator can be expressed as follows:

$$\begin{bmatrix} e_a \\ e_b \\ e_c \end{bmatrix} = \begin{bmatrix} R_s & 0 & 0 \\ 0 & R_s & 0 \\ 0 & 0 & R_s \end{bmatrix} \times \begin{bmatrix} i_a \\ i_b \\ i_c \end{bmatrix} + \begin{bmatrix} L_s - M & 0 & 0 \\ 0 & L_s - M & 0 \\ 0 & 0 & L_s - M \end{bmatrix} \times \frac{d}{dt} \begin{bmatrix} i_a \\ i_b \\ i_c \end{bmatrix} + \begin{bmatrix} v_a \\ v_b \\ v_c \end{bmatrix} \tag{1}$$

where e_x, v_x, i_x, R_s, L_s and M represent phase back-EMF voltage, terminal voltage, phase current, phase resistance, phase self-inductance, and mutual inductance, respectively.

The BLDC generator produces three-phase back-EMFs have trapezoidal shapes, as shown in Fig. 3, that the magnitudes are directly proportional to speed. The phase current shape of BLDC generator depends on the power conversion connected to generator and employed rectification strategy. To maximize the output power of BLDCG, an optimal current control strategy will be presented.

2.2. The power of BLDC generator

In the three-phase BLDC generator, the average airgap power is obtained from the following:

$$\begin{aligned} P_{avg} &= \sum_{k=a,b,c} \tfrac{1}{T} \int_0^T e_k(t) i_k(t) dt \\ &= \tfrac{1}{T} \int_0^T \{e_a(t) i_a(t) + e_b(t) i_b(t) + e_c(t) i_c(t)\} dt \\ &= \tfrac{3}{T} \int_0^T e_a(t) i_a(t) dt \end{aligned} \tag{2}$$

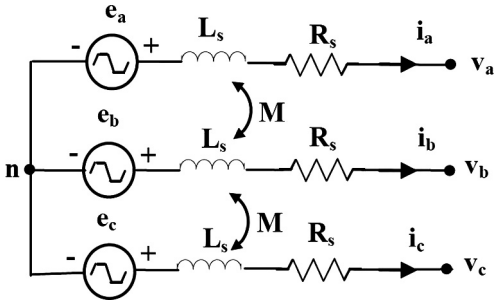

Figure 2 Equivalent circuit of BLDC generator.

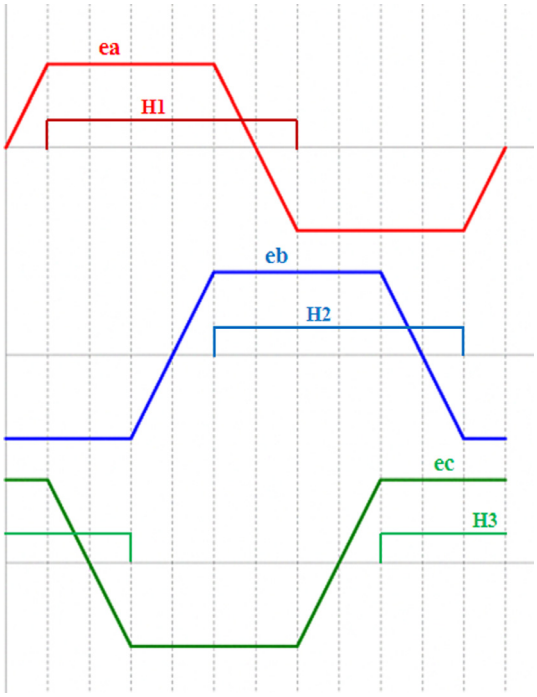

Figure 3 Back-EMF voltage waveforms and Hall Effect position sensors of BLDC generator with trapezoidal back-EMF waveforms.

where $e_k(t)$ represents the induced back-EMF phase voltage and $i_k(t)$ is the phase current of the generator. According to phase voltage equation (1), the output power of BLDC generator is calculated from the following:

$$\begin{aligned} P_{output} &= \sum_{k=a,b,c} \tfrac{1}{T} \int_0^T v_k(t) i_k(t) dt \\ &= \tfrac{3}{T} \int_0^T \left\{ e_a(t) - R_s \cdot i_a(t) - L_s \tfrac{di_a(t)}{dt} \right\} \cdot i_a(t) dt \\ &= \tfrac{3}{T} \left\{ \int_0^T e_a(t) \cdot i_a(t) dt - \int_0^T R_s \cdot i_a^2(t) dt - \int_0^T L_s \tfrac{di_a(t)}{dt} \cdot i_a(t) dt \right\} \\ &= \underbrace{\frac{3}{T} \int_0^T e_a(t) \cdot i_a(t) dt}_{\text{Airgap power}} - \underbrace{3R_s \cdot i_{a,rms}^2}_{P_{\text{loss}}} - \underbrace{\frac{3L_s}{T} \int_0^T i_a(t) di_a(t)}_{=0} \end{aligned} \tag{3}$$

It is observed that airgap power is composed of three components: output power, stator copper losses and average power of stator inductance that the latter is zero. Because the copper losses is a constant value in certain rms current and the average power of inductive component is null, so for optimal utilization of output power, maximization strategy can be onto components of airgap power.

2.3. Basic principle for maximization of the power of BLDC generator

The back-EMF voltages of BLDC generator are trapezoidal and for maximization of airgap power, trapezoidal phase current waveforms should be injected. It is resulted from that the airgap power is related to multiplying phase back-EMF voltage and current. If the phase current and voltage have the same shape, all harmonic components of voltages and currents

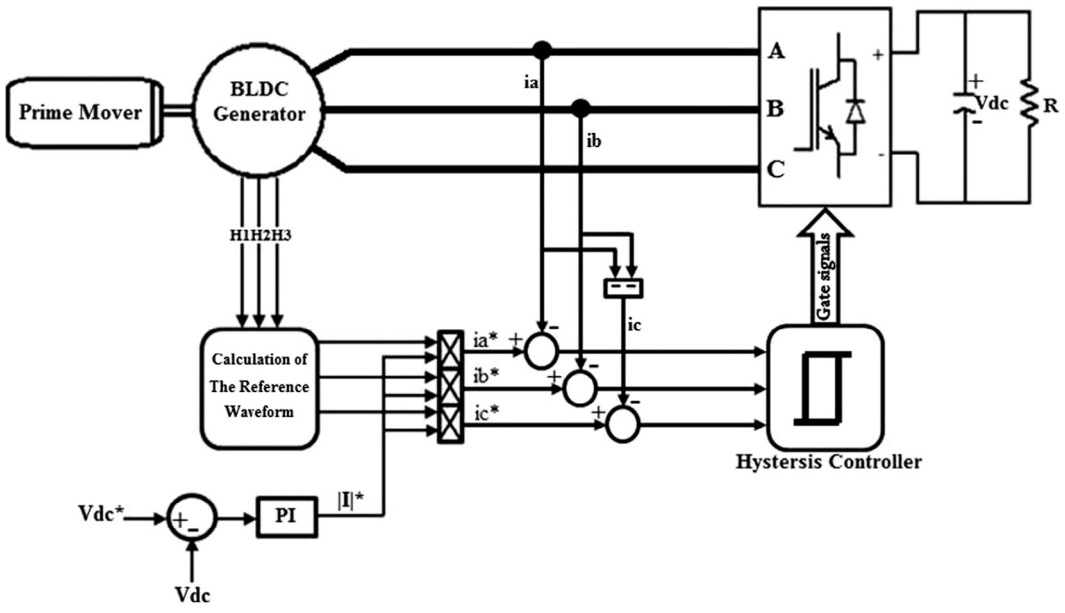

Figure 4 Brushless generator system topology with active rectifier to regulate the DC link voltage with maximization of the power.

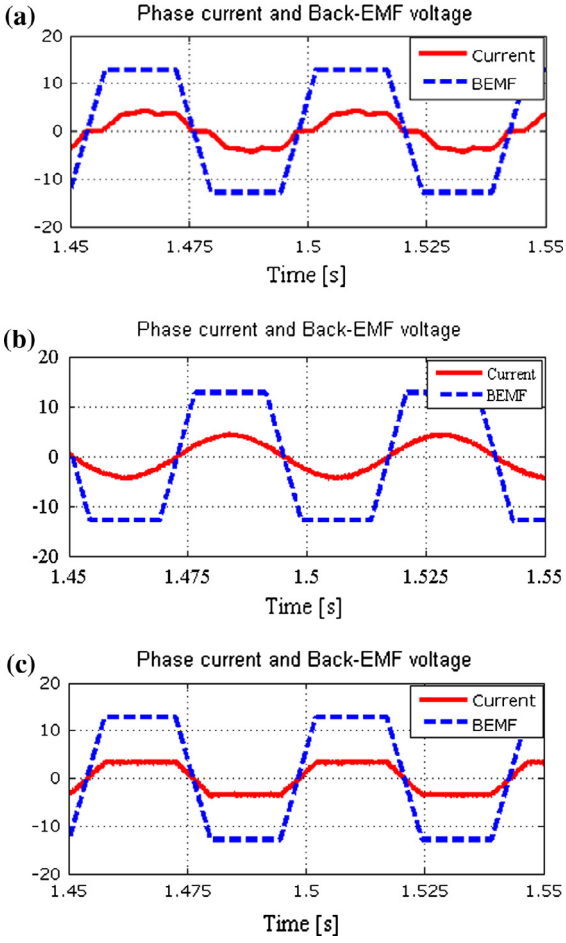

Figure 5 Induced back-EMF and phase current of BLDC generator at speed of 450 rpm at three cases: (a) use of full bridge diode rectifier, (b) use of active rectifier with sinusoidal and (c) trapezoidal reference current.

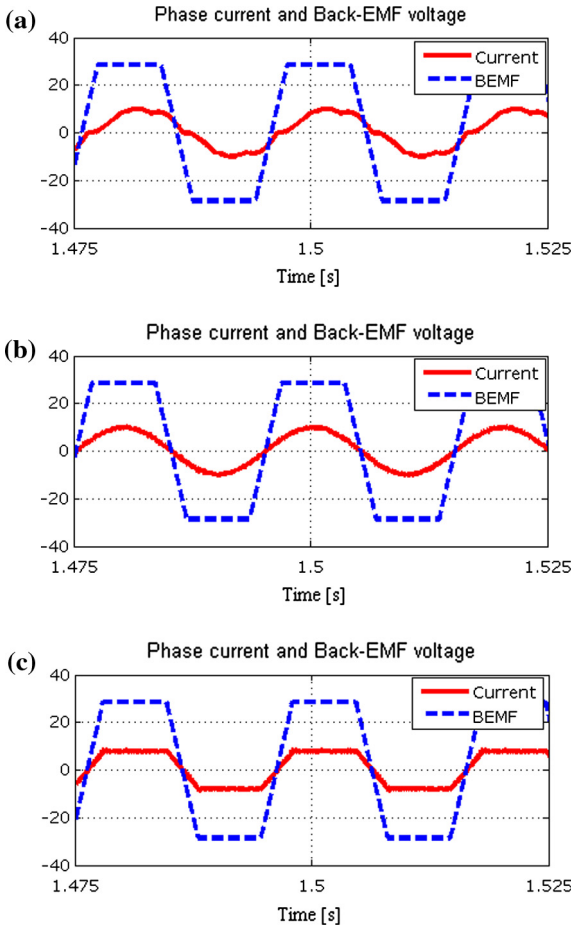

Figure 6 Induced back-EMF and phase current of BLDC generator at speed of 1000 rpm at three cases: (a) use of full bridge diode rectifier, (b) use of active rectifier with sinusoidal and (c) trapezoidal reference current.

Table 1 Comparison of power for BLDC generator.

	Full bridge diode rectifier	Hysteresis control		Full bridge diode rectifier	Hysteresis control	
		Trapezoidal	Sinusoidal		Trapezoidal	Sinusoidal
Speed (rpm)	450	450	450	1000	1000	1000
Rms current (A)	3	3	3	7	7	7
Power (W)	95.2	101.7	99.2	472.8	527.7	514
Increase (%)	–	6.8	4.2	–	11.6	8.7

will generate the power. Another point is that, phase voltage and current should be inphase. So, the following technique is based on the current control as a trapezoidal and in phase with the voltage. This philosophy is true for PM synchronous generator too. So, to maximize the power for PMSG, due to sinusoidal induced voltage in the stator windings, the best waveform for the current is sinusoidal inphase of voltage.

2.4. Reference current waveform generation

For power maximization of BLDC generator based on phase current control shaping, it is necessary to make the reference current waveforms. For comparison, three reference currents shapes: square, sinusoidal and trapezoidal are considered and are injected through the BLDCG's phases. The current shape that leads to the maximum power is introduced as optimal current. To make the trapezoidal waveform for the reference current in phase with voltage, a new technique is carried out based on the Hall Effect position sensors signals and costly shaft encoder is not needed. The magnitude of reference current is identified from requested power as written in (2). In Fig. 3, when the positive flat part of back-EMF voltage in phase A (e_a) tends to begin, the sensors states are as $H_1 = 1$ and $H_2 = 0$ and when e_a reaches to negative flat part, they are as $H_1 = 0$ and $H_2 = 1$. The negative slope part of trapezoidal reference current of phase a can be derived from the following:

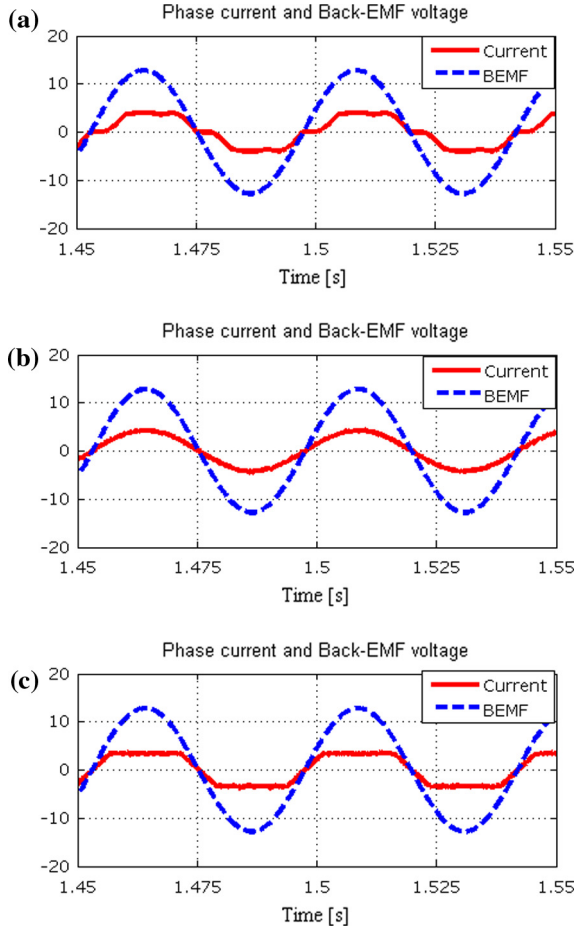

Figure 7 Induced back-EMF and phase current of PM synchronous generator at speed of 450 rpm at three cases: (a) use of full bridge diode rectifier, (b) use of active rectifier with sinusoidal and (c) trapezoidal reference current.

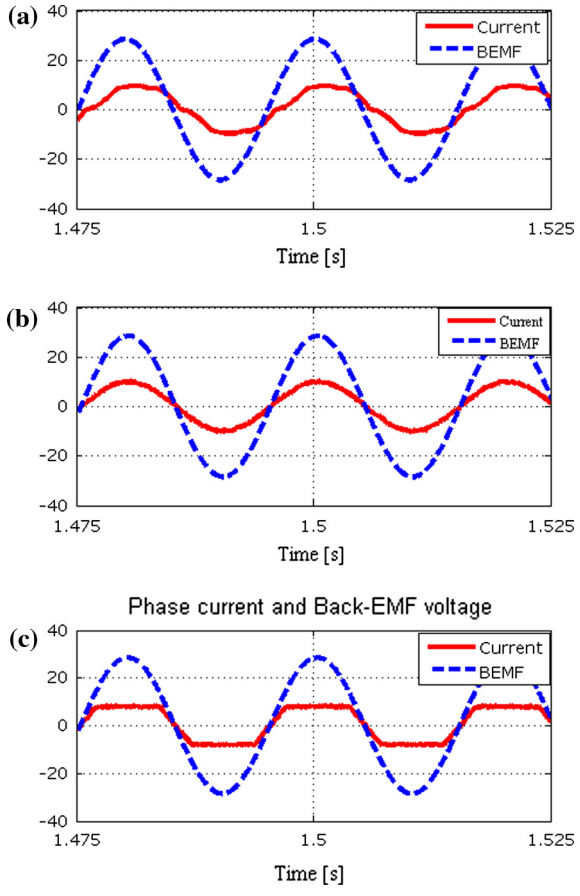

Figure 8 Induced back-EMF and phase current of PM synchronous generator at speed of 1000 rpm at three cases: (a) use of full bridge diode rectifier, (b) use of active rectifier with sinusoidal and (c) trapezoidal reference current.

Table 2 Comparison of power for PM synchronous generator.

	Full bridge diode rectifier	Hysteresis control		Full bridge diode rectifier	Hysteresis control	
		Trapezoidal	Sinusoidal		Trapezoidal	Sinusoidal
Speed (rpm)	450	450	450	1000	1000	1000
Rms current (A)	3	3	3	7	7	7
Power (W)	78.1	79.5	81.5	384.1	413	423.3
Increase (%)	–	1.8	4.3	–	7.5	10.2

$$I'_a - 1 = \frac{-2}{t_{H_2,on} - t_{H_1,off}}(t - t_{H_2,on}) \tag{4}$$

where $t_{H_2,on}$ and tH_1, off are the rising edge instant of sensor H_2 and the falling edge instant of sensor H_1 respectively. With the same manner, positive slope part of trapezoidal reference current of phase a can be derived. So, to make the whole trapezoidal phase reference current in phase with back-EMF voltage the following relation can be used:

$$\begin{cases} \text{if } H_1 = 1 \,\&\, H_2 = 0 \rightarrow I'_a = 1 \\ \text{if } H_1 = 1 \,\&\, H_2 = 1 \rightarrow I'_a = \frac{-2}{t_{H_2,on} - t_{H_1,off}}(t - t_{H_2,on}) + 1 \\ \text{if } H_1 = 0 \,\&\, H_2 = 1 \rightarrow I'_a = -1 \\ \text{if } H_1 = 0 \,\&\, H_2 = 0 \rightarrow I'_a = \frac{2}{t_{H_2,off} - t_{H_1,on}}(t - t_{H_2,off}) - 1 \end{cases} \tag{5}$$

The similar relations can be written to make trapezoidal reference currents for two phases B and C.

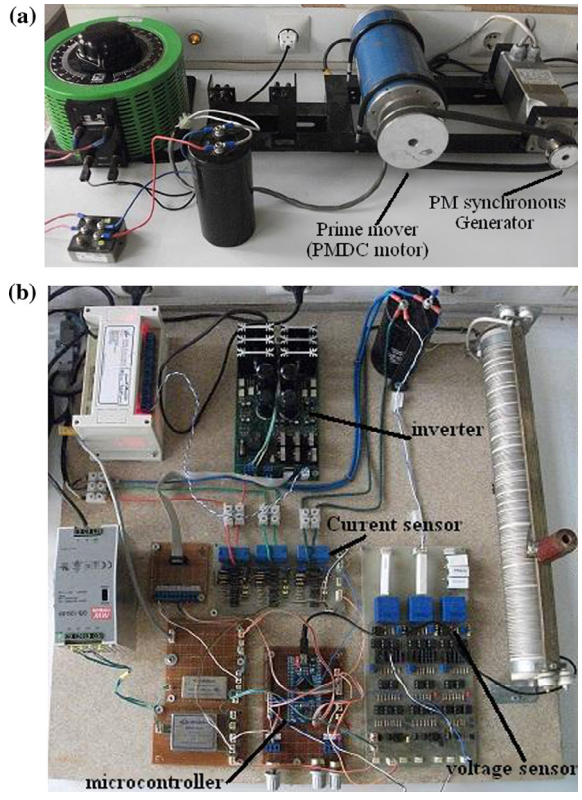

Figure 9 Experimental test-bed (a) PM synchronous generator and prime mover and (b) control system and load.

3. Simulation results

The proposed control to maximize the output power is verified via some simulations. Fig. 4 shows the topology of power generation system. The brushless generator is coupled via a PMDC motor as prime mover and is connected to an active three-phase rectifier to deliver the DC power to DC link and resistive load. The rectifier is controlled to capture the maximum power without any reactive power and maintain the DC link voltage at the desired level. With respect to the error between reference and actual voltages of DC link, PI controller develops magnitude of reference current. Due to the shape of

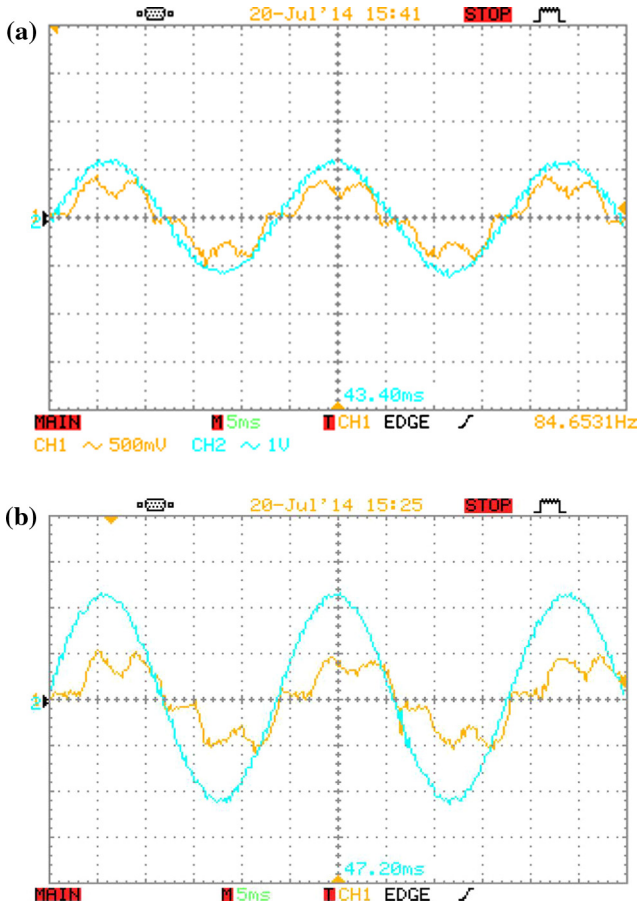

Figure 10 Phase back-EMF voltage and current waveforms when using the full bridge diode rectifier (a) at speed of 450 rpm and (b) at speed of 1000 rpm.

Table 3 Experimental results for PM synchronous generator.

	Full bridge diode rectifier	Hysteresis control		Full bridge diode rectifier	Hysteresis control	
		Trapezoidal	Sinusoidal		Trapezoidal	Sinusoidal
Speed (rpm)	450	450	450	1000	1000	1000
Rms current (A)	3	3	3	7	7	7
Power (W)	73	74.3	76	328	352.2	360.8
Increase (%)	–	1.7	4.1	–	7.3	10

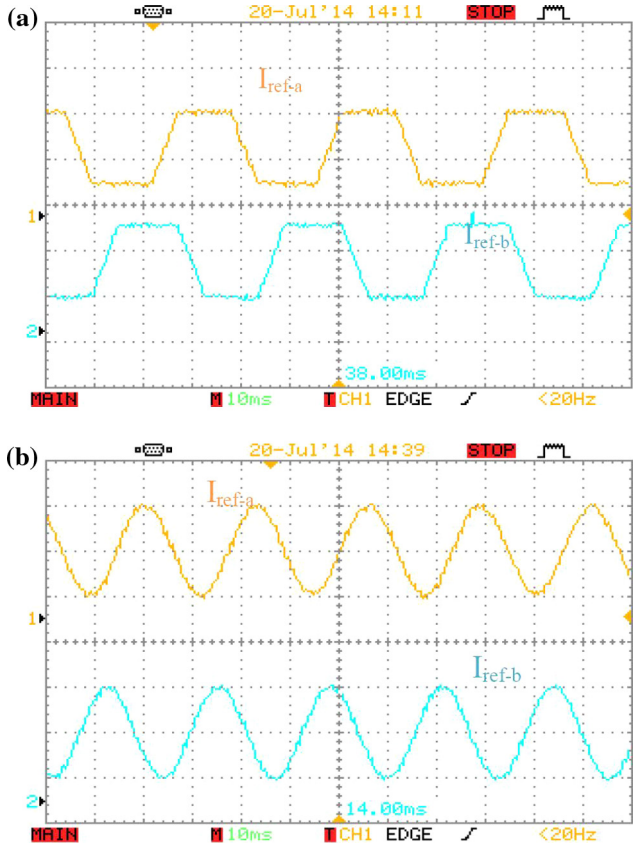

Figure 11 Created reference current waveforms in microcontroller (a) trapezoidal current and (b) sinusoidal current.

back-EMF voltage of brushless generator (trapezoidal or sinusoidal), the reference currents of three-phases are generated with the same phase of back-EMF voltages. Three hysteresis current controllers are employed to make the switching signals applied to active rectifier. As mentioned previously, for BLDC generator, trapezoidal reference current is made using Hall Effect position sensors signals, whereas for PMSG, shaft encoder is needed. The simulations are carried out for both BLDCG and PMSG. For each machine, the output powers in three cases corresponding to three different shapes of the reference currents are compared. These cases include (a) with passive rectifier, (b) active rectifier with sinusoidal current reference and (c) active rectifier with trapezoidal current reference. For better comparison, the output power of generator is calculated under same speed, load, and stator RMS current (or the same stator copper and rotational losses).

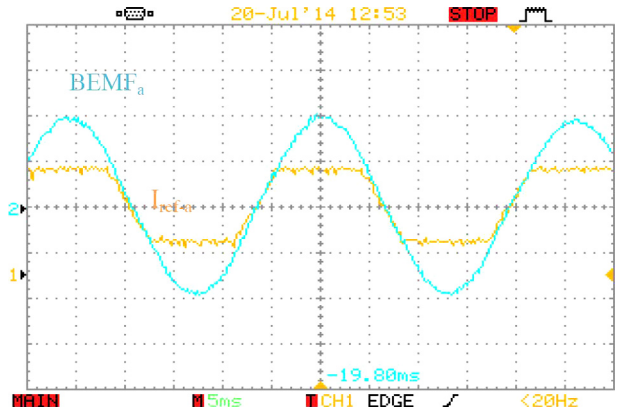

Figure 12 Phase current reference and back-EMF voltage waveforms.

Fig. 5 shows the simulation results including trapezoidal phase back-EMF voltage and current waveforms for BLDC generator under mentioned three cases at speed of 450 rpm. In the first case, when using full bridge diode rectifier as AC/DC converter for BLDC generator, the current waveform depends on the speed and load. Because the current is not controlled, it has some distortion due to effect of phase delay caused by phase inductance. So, the efficiency is low in this topology. In the second case, sinusoidal reference current is applied and produced via hysteresis controller. This current waveform cannot be favorable because all harmonic components of voltage and current are not involved to produce the power. In the third case, the trapezoidal shape phase currents are produced by BLDC generator using the hysteresis controllers. Since, the voltage and current have identical shape, so all harmonic components involve producing the power. The current distortion increases at higher speed for all three cases as shown in Fig. 6 due to more delay caused by inductance. The numerical results of BLDCG are summarized in Table 1. At speed of 450 rpm, with trapezoidal current reference, the generator power increases to 6.8% compared to full bridge diode rectifier and at speed of 1000 rpm it increases to 11.6%. At higher speed, the power increment will be more due to out-of-phase phenomenon between voltage and current. At any speed, the power of trapezoidal current is more than that of sinusoidal current.

The same simulation and analysis have been carried out for PMSG. Fig. 7 shows the simulation results of PMSG for passive and active rectifiers with sinusoidal and trapezoidal reference current waveforms at speed of 450 rpm. Since the induced back-EMF voltage is sinusoidal, it is expected that

sinusoidal waveform to be the optimal current waveform. The simulation results for PMSG at speed of 1000 rpm are shown in Fig. 8. There is considerable current distortion while using the passive rectifier and it increases at higher speeds. The numerical results for PMSG are summarized in Table 2. At the speed of 450 rpm, with applying the sinusoidal current the power of generator is 4.3% comparing to use of the full bridge diode rectifier. This increment reaches to 10.2% at speed of 1000 rpm. For trapezoidal reference current, the power increment is 1.8% and 7.5% at speeds of 450 rpm and 1000 rpm respectively that are less than sinusoidal case. It is noted the RMS current and so the stator copper loss is kept constant.

4. Experimental results

To validate developed control method and verification of presented simulations and analysis, an experimental test-bed has been designed and implemented. Fig. 9 shows the overall experimental setup system. A PMDC motor is used as prime mover of the system in the left side of Fig. 9(a) and a three-phase PM synchronous machine is used as the generator. Unfortunately, due to lack of proper trapezoidal BLDC generator in our laboratory, the experimental results are given just for PMSG. The input power or shaft speed of the generator may be varied via adjusting the PMDC's armature voltage. The specifications of PMSG and PMDC machines are given in Appendix A. As shown in Fig. 9(b), a three-phase active rectifier based on power MOSFETs is used and current and voltage Hall Effect sensors are used for current regulation and power calculation. A variable resistor is employed as electrical load. All the control and measurements are carried out via the low-cost microcontroller ATXMEGA128A3U.

At first, a full bridge diode rectifier is connected to PMSG. Fig. 10 shows the phase voltage and current waveforms of generator at two different speeds. There is no control on the current, and so phase voltage and current of PMSG are not inphase and this is more evident at high speeds. Some calculations of different practical results are summarized in Table 3. The trapezoidal and sinusoidal shaped reference current is made in the microcontroller as shown in Fig. 11. To make the trapezoidal, from Eq. (4), Hall Effect position sensors can be used, whereas to make the exact and inphase sinusoidal reference current, the shaft encoder should be used. Fig. 12 shows that the trapezoidal reference is perfectly in phase with back-EMF voltage.

Now, the active rectifier is used. Figs. 13 and 14 show the current waveforms of generator for two cases trapezoidal and sinusoidal reference current respectively at two speeds of 450 rpm and 1000 rpm. The performance of hysteresis current regulators is satisfactory, and the phase current tracks its

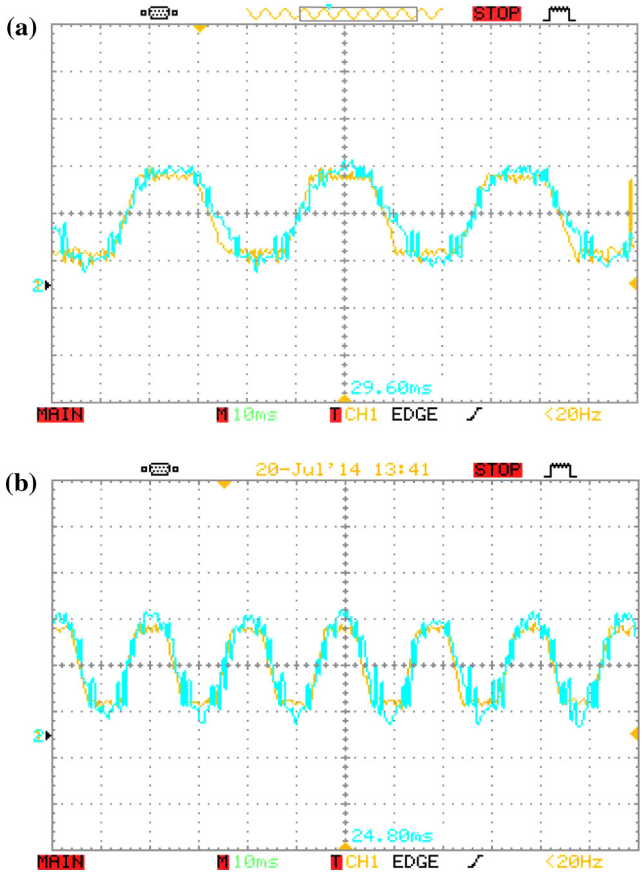

Figure 13 Trapezoidal reference and actual waveforms of phase current when using active rectifier (a) at speed of 450 rpm and (b) at speed of 1000 rpm.

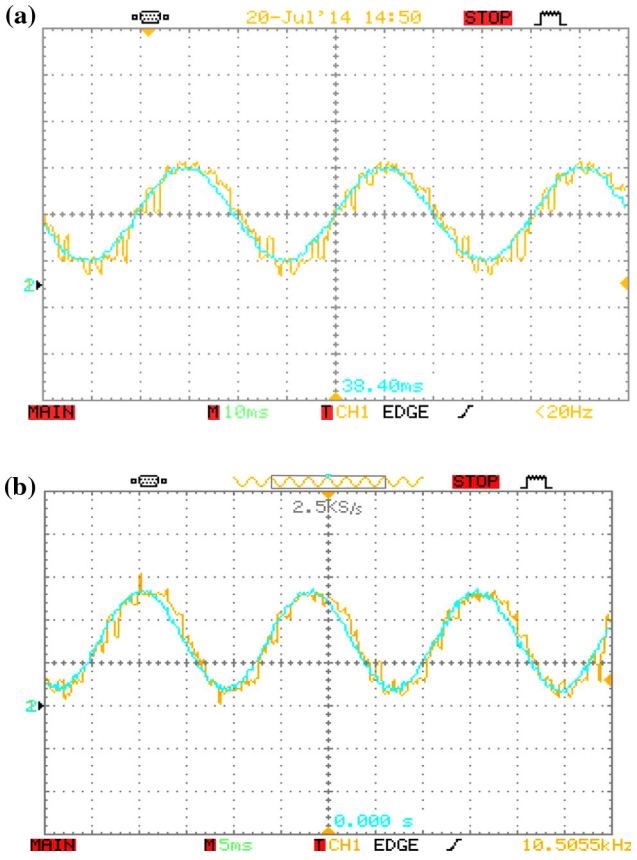

Figure 14 Sinusoidal reference and actual waveforms of phase current when using active rectifier (a) at speed of 450 rpm and (b) at speed of 1000 rpm.

corresponding reference well in each case. The power measurement results of three mentioned cases are summarized in Table 3. For each speed, the RMS current (stator copper loss) is kept constant. According to the given results, for sinusoidal reference current, at speed of 450 rpm power increases to 4.1% and at speed 1000 rpm, the power 10% is more than using the full bridge diode rectifier. At all speeds, the power increment of sinusoidal waveform is more than trapezoidal case. There are some differences between the simulation and experimental results of Tables 2 and 3 that may be caused by inexact used data are simulations.

5. Conclusion

A control technique for maximizing power per amps and efficiency of the BLDC and PM synchronous generator has been presented. This method is based on the phase current control. Simulations were performed for both generators and the experiment for PM synchronous generator by a powerful microcontroller XMEGA. In both works, an increase in power per amps and efficiency is achieved. For BLDC generator, the optimal current waveform is trapezoidal and to make the trapezoidal reference current, Hall Effect position sensors are used instead of using costly shaft encoders. Simulation results show an increase of 11.6% in the output power. Therefore, the weight and volume of the generator can be reduced by 11.6% by using the optimal control method. The results also show an increase of 8.7% in the output power by using the sinusoidal waveform for phase current of BLDC generator. Experimental results for PM synchronous generator show an increase of 10% in the output power. This control scheme can be used in electric and hybrid electric vehicles in regenerative braking or for optimization of the engines operation that leads the engine to work in optimal region.

Appendix A

PM synchronous generator parameters			
P_n	1.26 (kW)	Z_p	2 (poles)
ω_n	1000 (rpm)	K_e	0.0285 (V/rpm)
R_s	1.05 (Ω)	J	1.03e−4 (kg m^2)
L_s	3.5 (mH)	M	0.5 (mH)

PMDC motor parameters			
P_n	1.8 (W)	ω_n	2220 (rpm)
R_a	4 (Ω)	V_a	180 (V)

References

[1] Milivojevic N, Krishnamurthy M, Emadi A, Stamenkovic I. Theory and implementation of a simple digital control strategy for brushless DC generators. IEEE Trans Power Electron 2011;26(11):3345–56.

[2] Hendershot JR, Miller TJE. Design of brushless permanent-magnet motors. UK: Oxford Magna Physics Publications; 1994.

[3] Friedrich G, Kant M. Choice of drives for electric vehicles: a comparison between two permanent magnet AC machines. IEE Proc Electric Power Appl 1998;145(3):247–52.

[4] Yedamale P. Brushless DC (BLDC) motor fundamentals, Report AN885. Microchip Technology Inc.; 2003.

[5] Krishnan R, Rim GH. Modeling, simulation, and analysis of variable-speed constant frequency power conversion scheme with a permanent magnet brushless dc generator. IEEE Trans Industr Electron 1990;37(4):291–6.

[6] Onar OC, Gurkaynak Y, Khaligh A. A brushless DC generator & synchronous rectifier for isolated telecommunication stations. In: Proc of IEEE international telecommunications energy conference, 18–22 October, Incheon, South Korea; 2009. p. 1–6.

[7] Bose BK. Power electronics – a technology review. Proc IEEE 1992;80(8):1303–34.

[8] Ching-Tsai P, Ting-Yu C, Fang E. A novel single stage step up/down AC/DC converter for small BLDC wind power generators. In: Proc of IEEE international conferences on power electronics and drive systems (PEDS), 5–8 December, Sydney, Australia; 2011. p. 861–6.

[9] Milivojevic N, Krishnamurthy M, Gurkaynak Y, Sathyan A, Lee Y-J, Emadi A. Stability analysis of FPGA-based control of brushless DC motors and generators using digital PWM technique. IEEE Trans Industr Electron 2012;59(1):343–51.

[10] Jiaqun X, Jie J, Haotian C. A controlled rectification method for automotive brushless DC generator with ultracapacitor energy storage. In: Proc of 16th IEEE international power electronics and motion control conference and exposition (PEMC), 21–24 December, Antalya, Turkey; 2014. p. 168–73.

[11] Lee HW, Kim TH, Ehsani M. Practical control for improving power density and efficiency of the BLDC generator. IEEE Trans Power Electron 2005;20(1):192–9.

[12] Niasar A Halvaei, Behzadi Shahrbabak M. Direct power control of brushless DC generator for automotive applications. In: Proc of 5th IEEE power electronics, drive systems and technologies conference (PEDSTC), 5–6 February, Tehran, Iran; 2014. p. 267–72.

[13] Lee HW, Kim TH, Ehsani M. Maximum power throughput in the multiphase brushless DC generator. IEE Proc Electric Power Appl 2005;152(3):501–8.

[14] Gatto G, Marongiu I, Perfetto A, Serpi A. Brushless DC generator controlled by constrained predictive algorithm. In: Proc of IEEE international symposium on industrial electronics (ISIE), 4–7 July, Bari, Italy; 2010. p. 1224–29.

[15] Beik O, Schofield N, Al-Adsani A. Variable speed brushless hybrid permanent magnet generator for hybrid electric vehicles. In: Proc of IEEE transportation electrification conference and expo (ITEC), 15–18 June, Dearborn, USA; 2014. p. 1–6.

[16] Adhikari N, Singh B, Vyas AL, Chandra A, Al-Haddad K. Modeling and control of stand-alone energy conversion system with PMBLDC generator. In: Proc of 38th annual conference on IEEE industrial electronics society (IECON), 25–28 October, Montreal, Canada; 2012. p. 1085–90.

[17] Laczko AA, Zaharia MV, Radulescu MM, Brisset S. Modeling and simulation of a brushless DC permanent-magnet generator-based wind energy conversion system. In: Proc of IEEE international conference on ecological vehicles and renewable energies (EVER), March 31–April 2, Monte-Carlo, Monaco; 2015. p. 1–7.

Abolfazl Halvaei Niasar (S'04–M'06–SM'14) was born in Kashan, Iran in 1974. He received his B.Sc., M.Sc., and Ph.D. in 1996, 1999, and 2008 from Isfahan University of Technology (IUT), University of Tehran (UT) and Iran University of Science and Technology (IUST) respectively, all in electrical engineering. He has joined the Department of Electrical and Computer Engineering at University of Kashan, Kashan, Iran since 2008 as assistant professor. He has authored more than 80 technical papers published in journals and conference proceedings. He is the holder of two Iranian patents and has directed eight industrial research projects. His current major research interests include PM and brushless DC motor (BLDC) drives, sensorless drives, design, analysis and control of electrical machines, development of electric vehicles (EVs) and hybrid electric vehicles (HEVs), DSP based control systems and industrial control systems engineering. Dr. Halvaei is senior member of the Institute of Electrical and Electronics Engineers, IEEE.

AmirHossein Sabbaghean was born in Kashan, Iran in 1989. He received the B.Sc. from University of Kashan, Kashan, Iran in 2012 and M.Sc. from University of Kashan, Iran in 2015. His research interests are digital design implementation, ac and BLDC motor drives, power electronics.